J Sol-Gel Sci Technol (2017) 83:518–526
DOI 10.1007/s10971-017-4458-0

ORIGINAL PAPER: FUNCTIONAL COATINGS, THIN FILMS AND MEMBRANES (INCLUDING DEPOSITION TECHNIQUES)

Anti-reflection OTS-treated SiO_2 thin films with super-hydrophobic property

Hong Li[1] · **Naiyi Li**[1] · **Yanwen Zhang**[1] · **Huiting He**[1] · **Zirui Liu**[2]

Received: 12 May 2017 / Accepted: 19 June 2017 / Published online: 29 June 2017

Abstract Synthesizing multifunctional films to apply to the glasses for optical and advanced engineering applications, especially for concentrating solar power application, is a severe challenge. Herein, we report an anti-reflection SiO_2 thin films with super-hydrophobic property. The SiO_2 thin films are successfully synthesized on the soda lime glass by sol-gel spin-coating method, using tetraethylorthosilicate as a precursor and octadecyltrichlorosilane as a modification agent. The properties of films were characterized by fourier transform infrared spectra, field emission scanning electron microscopy, UV–VIS–NIR spectrophotometer and water contact angles apparatus. The results indicate that anti-reflection SiO_2 thin films have excellent visible light transmittance ranging from 97.8 to 103.4% with treatment time in tetraethylorthosilicate solution increasing from 1 min to 3 h. Moreover, such film exhibits super-hydrophobic property with water contact angles of 150.6° when treatment time is 3 h, owning to a hierarchical structure of the SiO_2 nanoparticles (~50 nm) and microscale dendritic aggregates. Fortunately, anti-reflection octadecyltrichlorosilane-treated SiO_2 films with super-hydrophobic property display a promising application in various fields, especially in concentrating solar power for reducing specular reflectance efficiency.

Graphical abstract

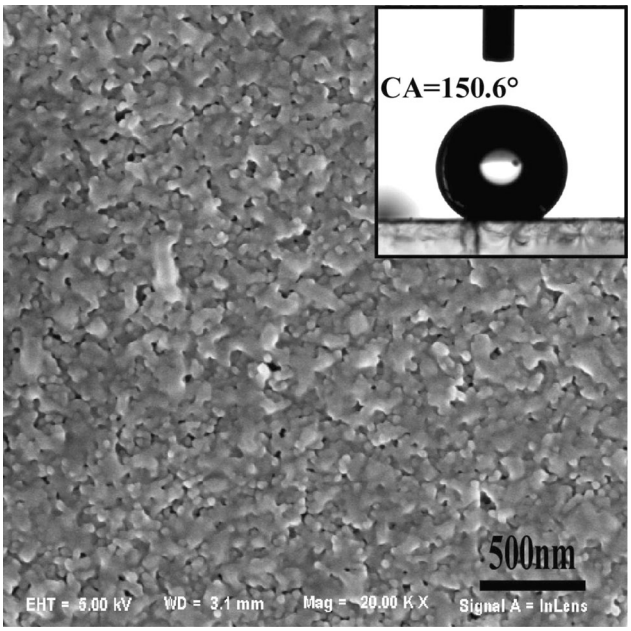

Keywords Anti-reflection · SiO_2 films · OTS · Super-hydrophobic property · Sol–gel

1 Introduction

Glasses are widely applied to various fields and offer many desirable properties, including optical clarity and overall visual appearance. The reduction in light reflection from the surface of a glass substrate may be desirable for routine applications, such as building glasses, windscreens, video display panels, flat-panel displays, photodetectors, infrared

✉ Hong Li
lh_648@whut.edu.cn

[1] State Key Laboratory of Silicate Materials for Architectures of Wuhan University of Technology, Wuhan 430070, China

[2] Department of Materials Science and Engineering, University of California, Los Angeles, CA 90095-1595, USA

sensors and lenses as well as for advanced engineering applications [1–4]. Therefore, coating of an anti-reflection layer emerges as required. Righeira [5] had designed novel multifunctional coatings that present anti-reflection, scratch, and abrasion resistance properties. That was achieved by a coating structure with a composite top layer comprising at least one type of metal oxide (ZrO_2 or TiO_2) or silane compound with low-refractive-index SiO_2 layer. However, since the enhancement of transmittance is selective toward specific wavelengths, the coating exhibits a high transmittance only in a narrow wavelength range [6]. As such, broadband anti-reflection coatings are highly desired to achieve an optimal performance. Lei [7] revealed a visible wavelength-independent anti-reflection coating generated from assembled SiO_2 particles modified with tetraethoxysilane. The resulted coating surface morphology resembled moth-eye-like nanostructure that exhibited visible wavelength-independent transmittance enhancement for substrate.

Apart from anti-reflection, the wettability is also a very important property of glass surfaces, which is governed by both the chemical composition and geometrical microstructure of the surfaces [8]. The two necessary conditions of the preparation of super-hydrophobic solid surface included low energy surface and special micro surface roughness [9, 10]. In particular, many researches had been done to investigate the super-hydrophobic biological surfaces [11, 12], especially the surface of lotus leaves [13]. The leaf of the Lotus plant achieved super-hydrophobic property using a hierarchical structure with roughness on both the microscale and nanoscale. Daniel [14] had presented a hierarchically structured surfaces with Lotus-effect properties using micro-sized and nano-sized hydrophobic silica particles and a simple spray method. The above results expounded that roughness increase due to existence of the micro-structure and nano-structure on the surface, which will further be conducive to the super-hydrophobic property. Besides these physical approaches, the modification of rough surfaces is another way to promote super-hydrophobic behavior [15–18]. Li [19] found that oleic acid-modified SiO_2 nanoparticles were capable of dispersing through esterification. In study of Jeong [20], hydrophobic porous silica has been prepared by surface modification of TEOS (tetraethylorthosilicate) wet gel with 6 and 12 vol.% of trimethylchlorosilane. The results indicated that modified dried gels had a surface area of 950–1000 m^2/g (average pore size 120 Å), compared to the non-modified surface which had a surface area of 690 m^2/g (average pore size 36 Å).

Much has been reported for modification agent. It is well-known that fluorine is effective for lowering the surface free energy chemically because fluorine has a small atomic radius and the biggest electronegativity among atoms, so it forms a stable covalent bond with carbon. Takashi [21] found that the dynamic contact angle (CA) of water on its surface was 119°, which corresponds to a surface free energy of 6.7 mJ/m^2. This value was considered to be the lowest surface free energy of any solid, based on the hexagonal closed alignment of $-CF_3$ groups on the surface. Xiu [22] proposed that after treating the film surface with a fluoroalkylsilane, the surface became super-hydrophobic with a CA near 170° and a CA hysteresis < 10°. Nevertheless, fluoride modification agent is too expensive to apply to various fields. Guo [23] described a super-hydrophobic silica film prepared by means of Sol–gel and self-assembly techniques, with a very high water CA (155–157°) and a small sliding angle (3–5°) after being modified with perfluorooctyltrichloromethoxysilane. This result could be ascribed to dramatically decrease of surface energy due to the existence of chloride on film surface, which presented similar electron-shell structure and electronegativity.

In the present study, we present anti-reflection OTS-treated SiO_2 thin films with super-hydrophobic property. Although some researchers have investigated the super-hydrophobic SiO_2 films modified with OTS, there are four highlights in this article as follow: (1) comparing to the current studies, we have given a better understanding of the formation of SiOH groups on SiO_2 films surface and the schematic of covalent bond formation between the OTS monolayer and the SiO_2 thin films, (2) Comparing to the published researches about transmittance (93.4–99.5%), these films present higher transmittance (97.8–103.4%) in visible region (400–800 nm), (3) when treatment time is 3 h, these films not only exhibit super-hydrophobic property with WCAs of 150.6° but also show excellent anti-reflection effect with transmittance of 97.8–100.9% in visible region and (4) these anti-reflection OTS-treated SiO_2 films with super-hydrophobic property present a promising application in various fields, especially in concentrating solar power (CSP) for reducing specular reflectance efficiency.

2 Experimental

2.1 Materials

In this work, TEOS ($C_8H_{20}O_4Si$, 93.2–93.6%), absolute ethanol (C_2H_5OH, purity >99.7%), ammonium hydroxide ($NH_3{\cdot}H_2O$, 36–38 wt%) and octadecyltrichlorosilane (OTS, $C_{18}H_{37}Cl_3Si$, purity > 95.0%) were used as the initial materials, supplied by Sinopharm Chemical Reagent Co. Ltd., China. Besides, soda lime silicate glasses (25 × 25 × 1 mm) were cut to use as substrates.

2.2 Preparation of OTS-SiO_2 composite thin films

SiO_2 thin films were successfully synthesized on soda lime glass substrates by sol–gel spin coating method shown in Fig. 1. Firstly, the gel was obtained by mixing absolute ethanol, ammonium hydroxide and TEOS, corresponding to the volume of 35, 2 and 2 mL, respectively. And then, the gel was spin-coated on the substrate once with a screw rotation rate of 750 rpm for 15 s and subsequently at 5000 rpm for 30 s. After being calcined at 200 °C for 60 min, SiO_2 thin films were gained. Finally, after being immersed in 20 mmol/L OTS solution for 0, 1/60, 3 and 15 h, respectively, and subsequently curing at 150 °C for 30 min, SiO_2 porous thin films were successfully modified with OTS.

2.3 Characterization

The Fourier transform infrared spectra of SiO_2 films before and after being modified with OTS for various time were recorded on a Fourier transform infrared spectrometer (FTIR, Nicolet6700, USA) in the frequency range from 4000 to 400 cm^{-1}. The surface morphology of SiO_2 films were observed by field emission scanning electron microscopy (FESEM, Zeiss Ultra Plus, Germany). The optical transmittance of SiO_2 films deposited on soda lime glass substrate were examined by a SHIMADZU UV-2550 spectrophotometer, from 300 to 800 nm. In particular, the transmittance of soda lime glass substrate is used as the baseline. The water contact angles (WCAs) of SiO_2 thin films were measured at ambient temperature by an automatic CA measure device (Dataphysics OCA35, Germany). Water droplets were generated automatically, with a volume of 5 μL. Typically, the average value of measurements at five different positions of the SiO2 thin films' surface was adopted as the value of the WCAs.

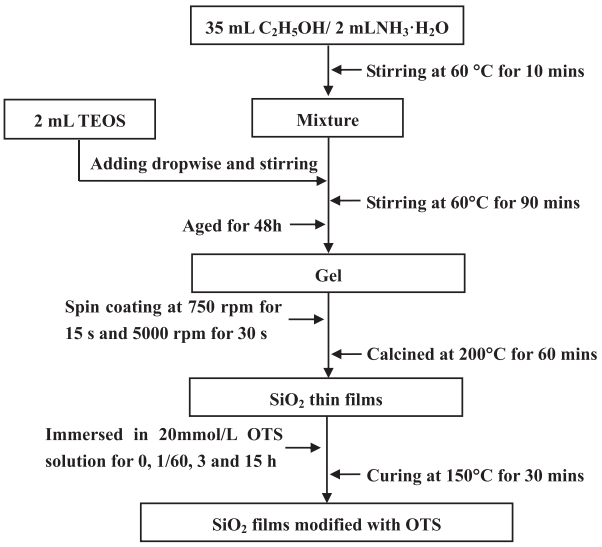

Fig. 1 Flowchart for synthesizing SiO_2 thin films

3 Results and discussion

3.1 FTIR analysis

Figure 2a–d are the FTIR spectrums of SiO_2 films after being modified with OTS for 0, 1/60, 3 and 15 h, respectively. Vibrational assignments and their corresponding frequencies are listed in Table 1 [24, 25]. Two main bands at 2851 cm^{-1} and 2921 cm^{-1} are clearly observed in the high frequency region [26] in Fig. 2b–d. These are assigned to the symmetric mode and asymmetric mode of $-CH_2$ of the OTS alkyl chains, separately. The peak frequencies for the $\nu_s(CH_2)$ and $\nu_a(CH_2)$ modes provide insight into alkyl chain packing in terms of crystallinelike or liquidlike structure. The peak frequency for the $\nu_a(CH_2)$ mode of an all-trans extended alkyl chain in a crystalline environment is reported to be ca. 2915–2921 cm^{-1}, and that for the $\nu_s(CH_2)$ mode is reported to be ca. 2846–2851 cm^{-1} [27, 28]. So the peak frequencies (2851 and 2921 cm^{-1}) observed for OTS are crystallinelike structure, suggesting that alkyl chains of

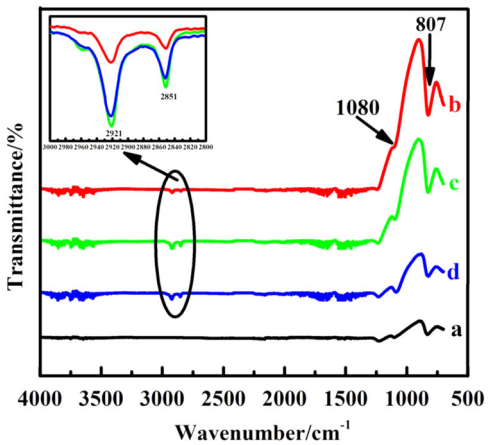

Fig. 2 FTIR spectra of SiO_2 films after being modified with OTS for various time: **a** 0 min, **b** 1 min, **c** 3 h, **d** 15 h

Table 1 FTIR peak frequencies and assignments for bonded OTS

Surface OTS[a]	Assignments[a,b]
807	ν_s(Si–O–Si)
1080	ν_a(Si–O–Si)
2851	$\nu_s(CH_2)$
2921	$\nu_a(CH_2)$

[a] In cm^{-1}

[b] ν stretch, *a* antisymmetric, *s* symmetric

OTS possess intermediate conformational order. Besides, the FTIR spectrums of all samples show absorption bands at 807 cm^{-1} and 1080 cm^{-1} in the high-frequency region (Fig. 2a–d) corresponding to symmetric vibration and asymmetric vibration of Si–O–Si, respectively [29]. This result indicates the formation of a cross-linked siloxane structure. Meantime, comparing to sample modified with OTS for 1 min, sample modified with OTS for 3 h presents more intense bands at both 2851 cm^{-1} and 2921 cm^{-1}, as shown in Fig. 2b, c. This result can be attributed to the fact that with increasing treatment time, siloxane bond formation has occurred not only between the OTS and SiO_2 surface silanols but also between at least a fraction of the head groups of the OTS molecules. However, in Fig. 2c, d, bands at both 2851 cm^{-1} and 2921 cm^{-1} are greatly similar, suggesting that SiO_2 films have been absolutely modified by OTS with modification time of 3 h. Therefore, when treatment time with OTS is over 3 h, the samples will present a similar bands at both 2851 cm^{-1} and 2921 cm^{-1}, because siloxane bond formation has occurred absolutely not only between the OTS and SiO_2 surface silanols but also the OTS molecules.

3.2 Surface microstructure

The SEM surface images of SiO_2 films after being modified with OTS for 0, 1/60, 3 and 15 h are shown in Fig. 3a–d, respectively. In Fig. 3a, SiO_2 films present a porous three-dimensional network structure without modifying with OTS. The network structure is formed by a series of microscale dendritic aggregates comprised SiO_2 nanoparticles. In particular, SiO_2 nanoparticles present a spheroidal structure with mean diameter of 50 nm. Xue [30] revealed that super-hydrophobic silica film was prepared by means of acid/base two step sol–gel and self-assembly techniques with tetraethoxysilane (TEOS) as precursor. The SiO_2 films, comprising SiO_2 nanoparticles (30–120 nm), had a high porosity with average pore size of 100–600 nm. And the porous structure was also formed by a series of dendritic aggregates comprised SiO_2 nanoparticles. This result is similar to that in this paper, due to the same preparation technique. In Fig. 3b, the dimension of dendritic aggregates of SiO_2 thin films increase after being modified with OTS for 1 min. Comparing to sample without modification, the mean diameter of SiO_2 nanoparticles after

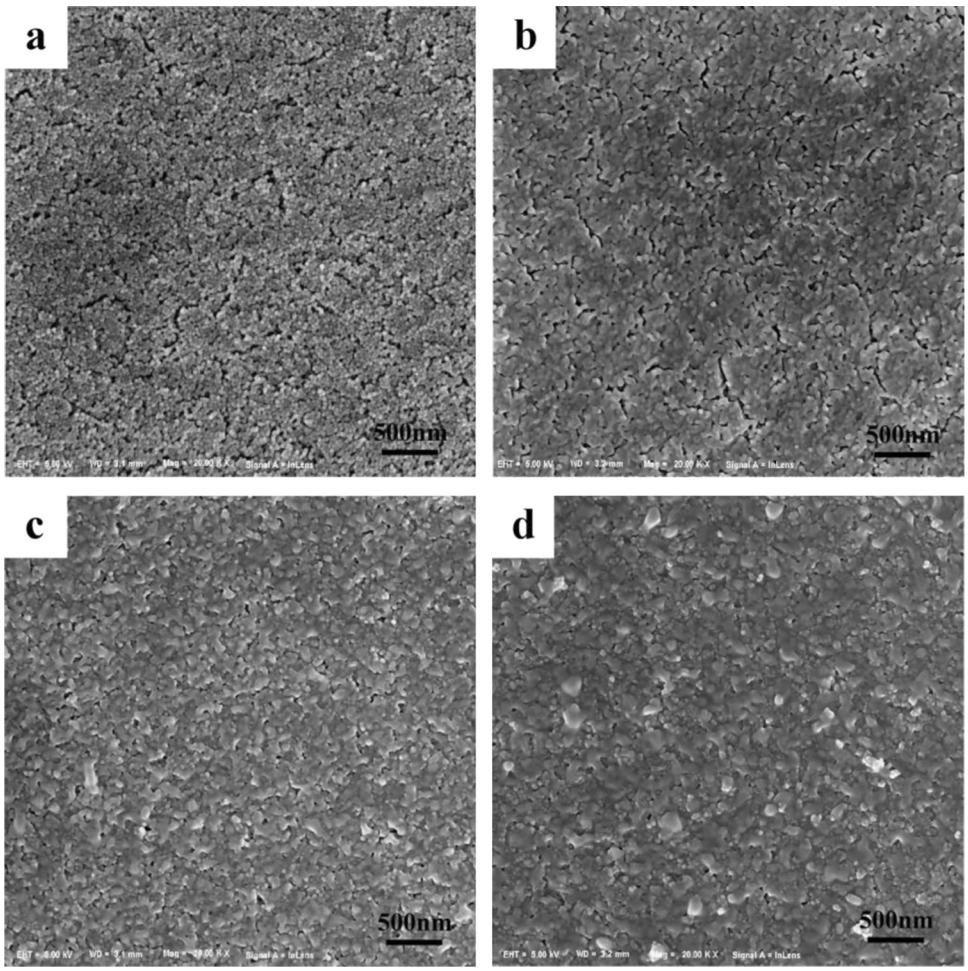

Fig. 3 The SEM surface images of SiO_2 films after being modified with OTS for various time: **a** 0 min, **b** 1 min, **c** 3 h, **d** 15 h

being modified with OTS for 1 min remains the same. Significant difference in surface structure is shown in Fig. 3a, b, due to the hydration of OTS and reaction between OTS and SiO_2 thin films surface. In Fig. 3c, the porosity of SiO_2 thin films with treatment time of 3 h decline, indicating that a self-assembled monolayer has nearly formed on the surface of SiO_2 thin films. This result is in accordance with that in Fig. 2c. Figure 3d presents the surface microstructure of the SiO_2 thin films modified with OTS for 15 h. It's obvious that mean diameter of SiO_2 nanoparticles remains the same but the dimensions of dendritic aggregates increase. The surface structure is more compact comparing with the sample while treatment time is 3 h, due to reaction not only between OTS and SiO_2 thin films surface but also the between head groups of the OTS molecules [28]. Moreover, the relationship between the relative amount of pores and the pore size for SiO_2 thin films modified with OTS for various reaction time, ranging from 0 to 15 h, is shown in Fig. 4. Without modifying with OTS, the pore size is mainly 35–55 nm (Fig. 4a). However, an obvious decline of the pore size can be seen in Fig. 4c (25–40 nm) and Fig. 4d (20–35 nm). Besides, the mean pore size of samples treated with OTS for 0, 1/60, 3 and 15 h decreases, corresponding to 44.63, 42.54, 34.14 and 27.93 nm, respectively.

In particular, the formation of SiOH groups on SiO_2 films surface and the schematic of covalent bond formation between the OTS monolayer and the SiO_2 thin films are demonstrated in Fig. 5a, b, respectively. As shown in Fig. 5a, the hydration chemistry of on high surface area silica (nanoparticles of SiO_2) occurs to form SiOH groups. Particularly, the silica surface can be dehydrated and rehydrated reversibly until a temperature of about 400 °C is reached, after which rehydration becomes extremely slow [31]. Meantime, hydrogen bonds occurs between the SiOH groups on the silica surface. Besides, physical absorption reaction happens between surface silanols and the water. Figure 5b shows the reactions between the OTS and SiO_2 surface. Firstly, hydration of OTS molecule takes place to form three silanol groups, because it contains three chlorine atoms, which can be hydrolyzed by trace water in solution [31]. Secondly, the dehydration reaction occurs between silanol group of OTS and SiO_2 films surface silanols, resulting in covalent bond formation between the monolayer and the SiO_2 film surface. Thirdly, OTS molecules crosslink to form polymeric species during film curing at 150 °C. Vapor-phase water can penetrate even a tightly packed, fully covered OTS surface, despite the hydrophobicity observed macroscopically. Water which penetrates the outer alkyl surface binds at the interfacial region to silanol groups attached to both the silica surface and the OTS molecules. Curing at 150 °C, which resulted in cross linking of organosilane molecules and covalent bond formation to the silica surface, decreases the number of silanol groups available for water adsorption. Thus, uncured OTS monolayers actually increase interfacial moisture adsorption relative to the unsilanized surface. After curing, water

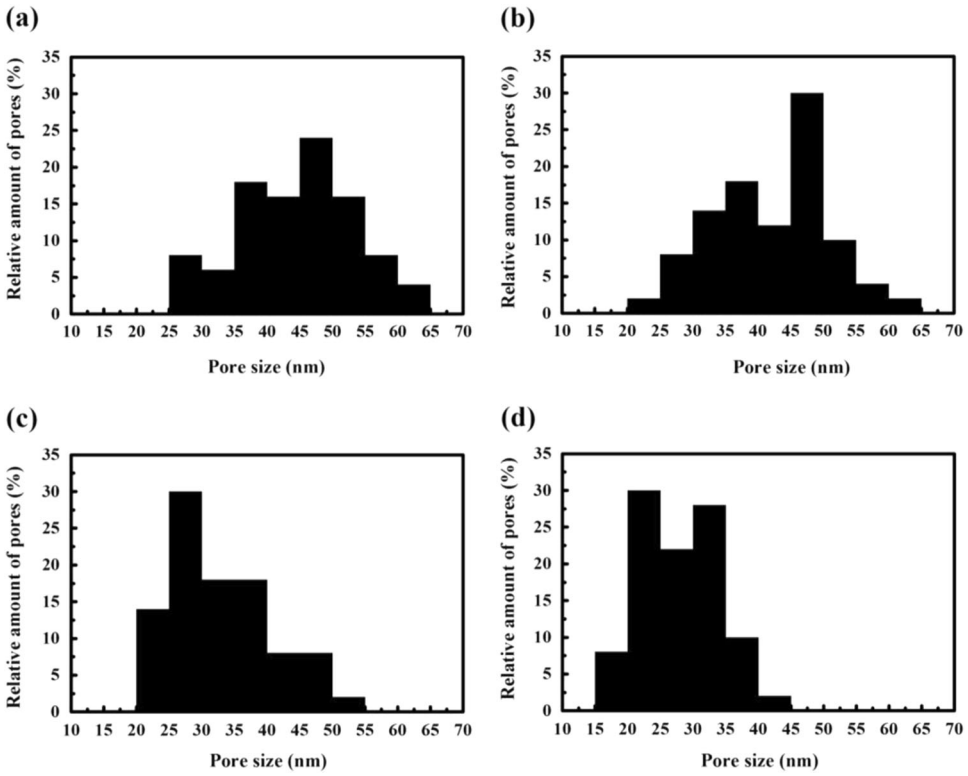

Fig. 4 The relative pore size distribution of SiO_2 films after being modified with OTS for various time: **a** 0 min, **b** 1 min, **c** 3 h, **d** 15 h

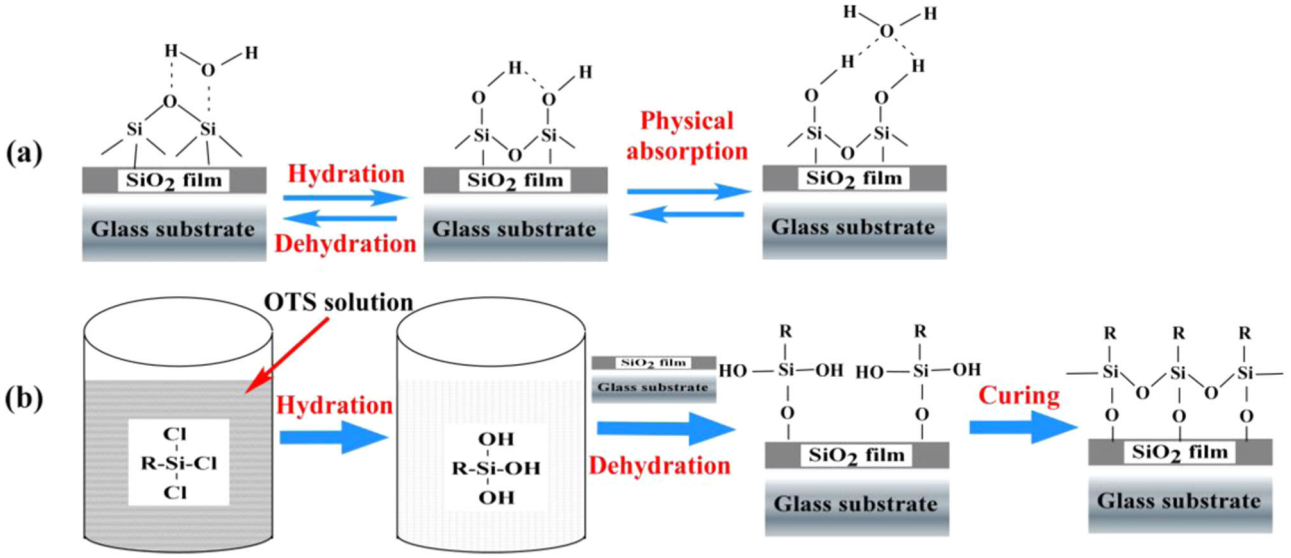

Fig. 5 The formation of SiOH groups on SiO_2 films surface (**a**) and the schematic of covalent bond formation between the OTS monolayer and the SiO_2 thin films (**b**). Hydrolysis of the chloride group by trace amounts of water in solution to silanol is followed by condensation with surface silanols, resulting in covalent bond formation between the monolayer and the substrate. Besides, OTS molecules can also cross-link to form polymeric species during film curing

absorption at the OTS/silica interface is greatly decreased, since the number of silanols present at the interface is reduced [32].

3.3 Transmittance

Figure 6 presents the optical transmittance of uncoated glass and SiO_2 films after being modified with OTS for 0, 1/60, 3 and 15 h. In particular, the transmittance of soda lime glass substrate is used as the baseline. As presented in Fig. 6a, the uncoated glasses have a high visible light (400–800 nm) transmittance, ranging from 88.4 to 90.3%. Fortunately, glass substrate with SiO_2 thin films without modifying with OTS exhibits a higher transmittance within visible region, ranging from 101.3 to 103.4% (Fig. 6b). The measurement optical transmittance exceeds 100%, indicating that the refractive indices of SiO_2 films is smaller than that of soda lime glass substrate. In this case, the SiO_2 thin films present excellent anti-reflection effect [33]. Anti-reflection films reduce the intensity of reflection and increase the quality of optical lens systems [5].

The basic principle of optical coatings can easily be understood as follow [34]. The reflected light from the air-film and film-substrate interfaces must interfere destructively to maximize the light transmission into the transparent substrate (Fig. 7). In this case, the light amplitudes reflected at both interfaces must be equal, that is,

$$n_f = \sqrt{n_o n_s}, \quad (1)$$

where with n_o, n_f, and n_s are the refractive indices of air, film, and substrate respectively. Besides, the optical path length must be chosen for the reflected wave to interfere destructively, namely, the film thickness must be 1/4 of a reference wavelength in the optical medium. In this experiment, the refractive indices of glass substrates n_s is 1.52. It is obvious that higher transmittance can be achieved when the refractive indices of films is closer to 1.23, according to Eq. (1). The prepared SiO_2 thin films present a porous structure (Fig. 3) due to the fact that the films are made up of a series of dendritic aggregates comprised SiO_2 nanoparticles synthesized via sol–gel spin-coating method. Such an appropriate porous structure is contributed to reduce the reflection and scattering to induce anti-reflection effect [35, 36]. The refractive indices of SiO_2 thin films n_f is close to 1.23, that is, the SiO_2 thin films present anti-reflection property [34].

From Fig. 6b, c we know that transmittance of SiO_2 films after being modified with OTS for 1 min is lower than that of the sample without OTS treatment, varying from 99.8 to 102.6%. Besides, comparing to the sample modified with OTS for 1 min, transmittance of SiO_2 films after being modified with OTS for 3 h decrease, but it is still so high, ranging from 97.8 to 100.9% (Fig. 6d). Nevertheless, transmittance of the sample modified with OTS for 15 h decline rapidly (Fig. 6e). In particular, in visible region (400–630 nm), transmittance is lower than that of the uncoated glass, as shown in Fig. 6a, e. Naganuma [37] had investigated the effect of glass particle size on the light transmittance of epoxy matrix composites, and found that reasonably controlling the glass particle size (porosity) can improve the light transmittance. In this paper, the transmittance decreases by increasing reaction time. This is

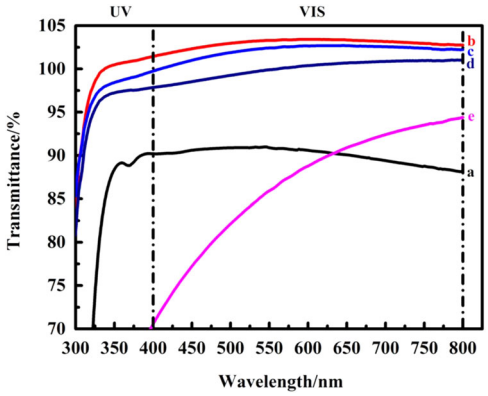

Fig. 6 Transmittance of uncoated glass and glasses with SiO_2 films after being modified with OTS for various time: **a** uncoated glass, **b** 0 min, **c** 1 min, **d** 3 h, **e** 15 h

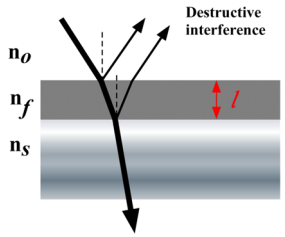

Fig. 7 Reflection of light from both air-film and film-substrate interfaces. For a given wavelength and incidence angle, light transmission is maximized when the two reflected beams interfere destructively

because anti-reflection effect of SiO_2 thin films gradually disappears resulting from the decline of porosity as presented in Fig. 3. After immersing in OTS solution, the self-assembled process occurs. The SiO_2 nanoparticles reunite to form dendritic aggregates and the aggregates gradually grow up. So the SiO_2 thin films become more compact by increasing reaction time, further resulting in decrease of porosity. Besides, when reaction time is too long, a monolayer of OTS would be formed on the surface of SiO_2 films (shown in Fig. 3d), resulting in increasing the thinness of the films. In this case, absorbance of visible light increases, leading to the decline of transmittance [6, 7].

3.4 Hydrophobic properties of SiO_2 films modified with OTS

The wettability [38] is omnipresent in nature and also plays a crucial role in various industrial processes. Importantly, the wettability depended on the surface chemical composition and roughness. Usually, the CA is used to assess the wettability. In this paper, the surface wettability of SiO_2 thin films after being modified with OTS for various time was investigated by measuring the WCAs on the surface of the thin films. Water droplets were generated automatically, with a volume of 5 µL. Typically, the average value of measurements at five different positions of the SiO_2 thin films surface was adopted as the value of the WCAs. The optical images of water spreading on the surface of SiO_2 thin films after OTS treatment for 0, 1, 30 and 180 min are shown in Fig. 8a–d, respectively. In Fig. 8a, WCA is 9.7°, indicating that SiO_2 film without OTS treatment presents a nice hydrophilic property. Nevertheless, in Fig. 8b, c, the samples exhibit hydrophobic property with WCAs of 117.1° and 131.6° while being treating for 1 and 30 min, respectively. In addition, when treatment time is 3 h, SiO_2 film shows super-hydrophobic property with WCAs of 150.6°.What's more, supplementary experiments have been done to investigate the effect of treatment time in OTS solution on WCAs, and the results are presented in Fig. 9. It is obvious that the more the treatment time, the larger WCAs. In particular, WCAs of the SiO_2 film rapidly increases and is close to the limiting value after ~3 h of immersion time. The final WCA of SiO_2 film is about 154.3°. This result in turn suggested that the OTS molecules have nearly reacted with the SiO_2 films surface when treatment time is 3 h.

According to the formation mechanism of the alkylsiloxane monolayers, the OTS molecules in the organic solvent can be gradually adsorbed onto a water layer present on SiO_2. Following physisorption, the trichlorosilane head groups are hydrolyzed to form trisilanols. Jae [39] proved that the silanols existed in a highly mobile hydrogen-bonded state. This led to important in-plane reorganizations of OTS molecules, thereby forming a uniform densely packed molecular island at the early stage of monolayer formation on the SiO_2 substrate. Silanol head groups of this island then became grafted to the SiO_2 substrate by irreversible cross linking to one another and covalent grafting to the substrate surface [40–42].

4 Conclusions

Anti-reflection SiO_2 thin films with super-hydrophobic property were successfully synthesized on the soda lime glass by sol–gel spin-coating method, using TEOS as precursor and OTS as modification agent.

1) Siloxane bond formation has occurred not only between the OTS and SiO_2 surface silanols but also between at least a fraction of the head groups of the OTS molecules, to from a cross-linked siloxane structure.
2) The SiO_2 films display a three-dimensional network structure formed by number of dendritic aggregates comprised SiO_2 nanoparticles with mean diameter of 50 nm. With increasing treatment time with OTS ranging from 0 to 15 h, mean diameter of SiO_2 nanoparticles remains the same but the dimensions of dendritic aggregates increase and porosity decline.

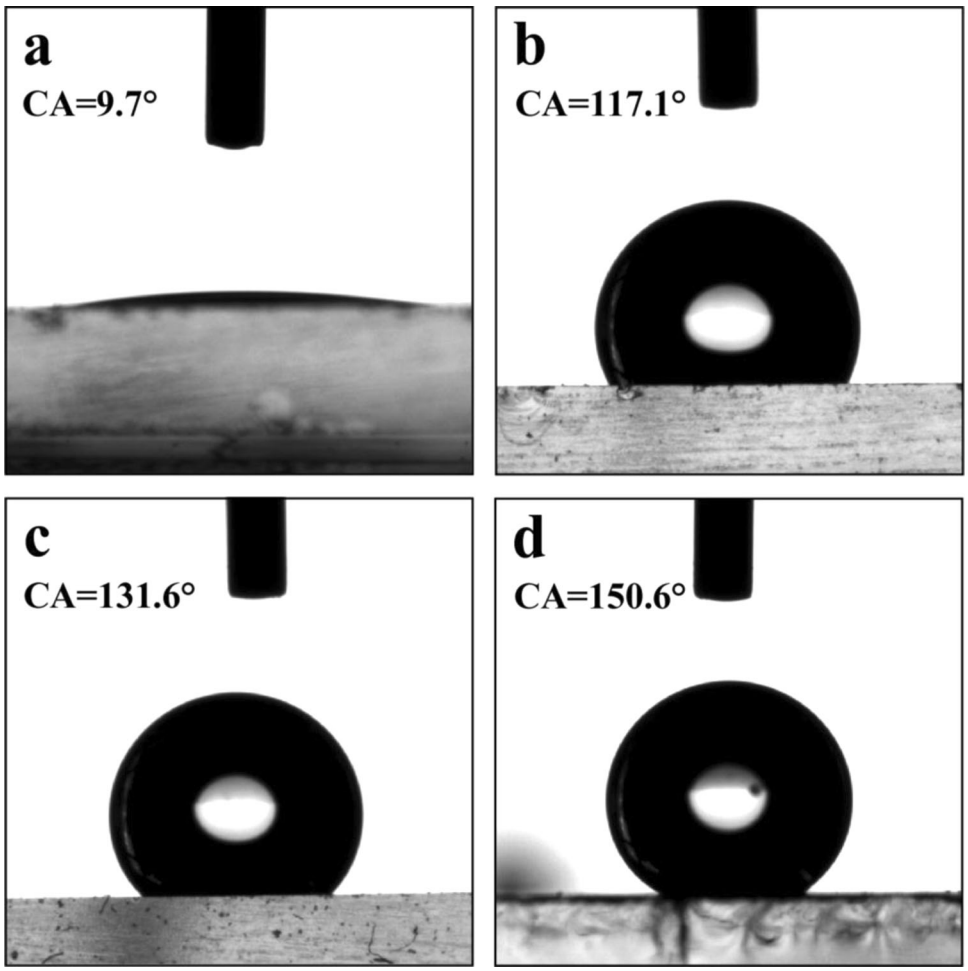

Fig. 8 The optical images of water spreading on the surface of SiO_2 thin films after OTS treatment for various time: **a** 0 min, **b** 1 min, **c** 30 min, **d** 180 min

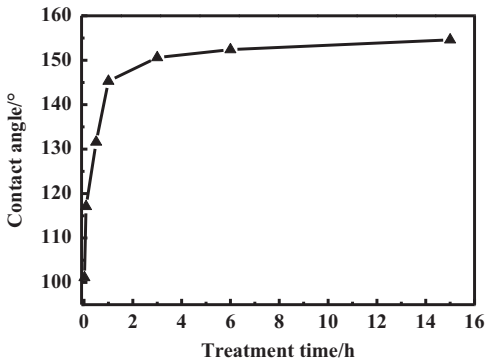

Fig. 9 The relationship between water contact angle and treatment time in OTS/n-hexane solution

3) As treatment time with OTS increase from 1 min to 3 h, the optical transmittance of glasses with SiO_2 thin films in visible light region (400–800 nm) decrease with a maximum value of around 103.4% and a minimum value of 97.8%, but is still drastically higher than that of uncoated glass, ranging from 88.4 to 90.3%. The results indicate that SiO_2 thin films exhibit excellent anti-reflection property.

4) The SiO_2 thin films present super-hydrophobic property with WCAs of 150.6° when treatment time is 3 h. Fortunately, anti-reflection OTS-treated SiO_2 films with super-hydrophobic property present a promising application in various fields, especially in CSP for reducing specular reflectance efficiency.

Acknowledgements The authors would like to express sincere thanks for the financial support from the National Natural Science Foundation of China (51372179), the Science and Technology Planning Project of Hubei Province (2014BAA136), the Hubei Province Foreign Science and Technology Project (2016AHB027).

Compliance with ethical standards

Conflict of interest The authors declare that they have no competing interests.

References

1. Lien SY, Wu DS, Yeh WC, Liu JC (2006) Sol Energy Mater Sol Cells 90:2710–2719

2. Chabas A, Lombardo T, Cachier H, Pertuisot MH, Oikonomou K, Falcone R, Verita M, Geotti-Bianchini F (2008) Build Environ 43:2124–2131
3. Prado R, Beobide G, Marcaide A, Goikoetxea J, Aranzabe A (2010) Sol Energy Mater Sol Cells 94:1081–1088
4. Xu X, Vignarooban K, Xu B, Hsu K, Kannan AM (2016) Renew Sustain Energy Rev 53:1106–1131
5. Carnegie MR, Sherine A, Sivagami D, Sakthivel S (2016) J Sol–gel Sci Technol 78:176–186
6. Li X, Gao J, Xue L, Han Y (2010) Adv Funct Mater 20:259–265
7. Yang L, Jiang H, Feng X, Shen Y, Jia L (2016) J Sol–gel Sci Technol 79:520–524
8. Lei F, Li S, Li Y, Li H, Zhang L, Zhai J, Song Y, Liu B, Lei J, Zhu D (2002) Adv Mater 14:1857–1860
9. Huang Y, Liu W, Luo G (2008) Polym Mater Sci Eng 24:13–16
10. Duan H, Xiong Z, Wang H, Zhao H, Gao D (2006) Chem Ind Eng 23:81–87
11. Barthlott W, Neinhuis C (1997) Planta 202:1–8
12. Koch K, Bohn HF, Barthlott W (2009) Langmuir 24:14116–14120
13. Ennaceri H, Alami HE, Brik H, Mokssit O, Khaldoun A (2014) Compos Mater Renew Energy Appl 10:1–4
14. Ebert D, Bhushan B (2012) J Colloid Interface Sci 368:584–591
15. Nuria G, Esperanza B, Julio G, Pilar T (2007) J Am Chem Soc 129:5052–5060
16. Zhang X, Shi F, Yu X, Liu H, Fu Y, Wang Z, Jiang L, Li X (2004) J Am Chem Soc 126:3064–3065
17. Nicolas M, Guittard F, Geribaldi S (2006) Langmuir 22:3081–3088
18. Guo M, Diao P, Cai S, Liu Z (2004) Chem J Chin Univ 25:547–549
19. Li Z, Zhu Y (2003) Appl Surf Sci 211:315–320
20. Jeong A-Y, Koo S-M, Kim D-P (2000) J Sol–gel Sci Technol 19:483–487
21. Nishino T, Meguro M, Nakamae K, Matsushita M, Ueda Y (1999) Langmuir 15:4321–4323
22. Xiu Y, Xiao F, Hess DW, Wong CP (2009) Thin Solid Films 517:1610–1615
23. Guo Z, Zhou F, Liu W (2006) Acta Chim Sci 64:761–766
24. Mirji SA (2006) Surf Interface Anal 38:158–165
25. Rouchon D, Rochat N, Gustavo F, Chabli A, Renault O, Besson P (2002) Surf Interface Anal 34:445–450
26. Abdelghani A, Hleli S, Cherif K (2002) Mater Lett 56:1064–1068
27. Mirji SA (2006) Colloids Surf A Physicochem Eng Asp 289:133–140
28. Cai M, Ho M, Pemberton JE (2000) Langmuir 16:3446–3453
29. Qasim M, Singh BR, Naqvi AH, Paik P, Das D (2015) Nanotechnology 26:1–14
30. Zai-lan X, Wu Y, Hao G, Li-yan C, Ai-Ju Z, Jin-zhang G (2008) J Northwest Norm Univ Nat Sci 44:65–69
31. Angst DL (1991) Langmuir 7:2236–2242
32. Oh T, Kim JW (2008) International conference on condition monitoring and diagnosis. 2008:276–279. doi:10.1109/CMD.2008.4580280
33. Jian M, Bingqi L, Wenshen H, Jun Y, Xinxin L (2009) Opt Tech 35:513–516
34. Walheim S, Schaffer E, Mlynek J, Steiner U (1999) Science 283:520–522
35. Yang D, Xu Y, Xu W, Wu D, Sun Y, Zhu H (2008) J Mater Chem 18:5557–5562
36. Zhang X-T, Sato O, Taguchi M, Einaga Y, Murakami T, Fujishima A (2005) Chem Mater 17:696–700
37. Naganuma T, Kagawa Y (1999) Acta Mater 17:4321–4327
38. Wang B, Feng J, Gao C (2005) Colloids Surf A Physicochem Eng Asp 259:1–5
39. Lee JP, Kim HK, Park CR, Park G, Kwak HT, Koo SM, Sung MM (2003) J Phys Chem B 107:8997–9002
40. Lercel MJ, Craighead HG, Parikh AN, Seshadri K, Allara DL (1996) J Vac Sci Technol A Vac Surf Films 14:1844–1849
41. Carson G, Granick S (1989) J Appl Polym Sci 37:2767–2772
42. McGovern ME, Kallury KMR, Thompson M (1994) Langmuir 10:3607–3614